Lepton Flavor Universality at Belle and Belle II

Seema Choudhury[1,*] (on behalf of Belle and Belle II collaborations)

[1]Iowa State University and High Energy Accelerator Research Organization

Abstract. We report the test of lepton flavor universality at Belle and Belle II experiments considering $b \to c$ and $b \to s$ transitions. We use 711 fb^{-1} and 189 fb^{-1} of data collected at $\Upsilon(4S)$ resonance from electron-positron collisions for Belle and Belle II, respectively. For the $b \to c$ transition, we present the measurement of lepton-flavor-universality in $B^0 \to D^{*-}\ell^+\nu_\ell$ decay, exclusive measurement of $\mathcal{R}(D)$ & $\mathcal{R}(D^*)$ in Belle data, and inclusive $R(X_{e/\mu})$ in Belle II. For the $b \to s$ transitions, we provide measurements of R_K and R_{K^*} using Belle data, measurement of the branching fraction for the decay $B \to K^*\ell\ell$, and test of lepton-flavor-universality in $B \to J/\psi K$ using Belle II data. Additionally, we report the lepton-flavor-universality in $\Omega_c^0 \to \Omega^-\ell^+\nu_\ell$ decay using 922 fb^{-1} of data collected by the Belle detector.

1 Belle and Belle II detectors

KEKB was an asymmetric energy e^+ (3.5 GeV) - e^- (8 GeV) collider with center-of-mass (CM) energy at the $B\overline{B}$ threshold corresponds to 10.58 GeV. Belle [1] detector was situated at the interaction point of the e^+e^-. It has collected 711, 89.5, and 121.1 fb^{-1} data at the CM energies 10.58, 10.52, and 10.86 GeV, respectively from 1999 to 2010. The detector consisted of many sub-detectors to identify different charged neutral particles. Belle II [2] is the successor of the Belle experiment with e^+ and e^- energies of 4 GeV and 7 GeV, successfully collecting data from 2019. It aims at collecting 50 ab^{-1} of data by 2035 and plans to deliver collision at a peak luminosity of 6.5×10^{35} cm^{-2}s^{-1} [2] (30 times that of KEKB). The increase in peak luminosity is contributed by the reduction in the beam size by 20 times and 1.5 times increase in beam current. The Belle II detector is also upgraded to cope-up with the beam background which increases in proportion to the luminosity. Belle II has collected $\sim$ 424 fb^{-1} data sample to date, having 362, 42, and 19 fb^{-1} at 10.58, 10.52, and 10.75 GeV, respectively. Belle II has a world record instantaneous luminosity of 4.71×10^{34} cm^{-2}s^{-1} on 22^{nd} June 2022.

2 LFU in $b \to c$ transition

The B decays with $b \to c$ tree-level transition are an important probe to test the lepton-flavor-universality (LFU). The ratio of exclusive decays with τ lepton can be used to test the standard model (SM) by measuring $\mathcal{R}(D^{(*)}) = \dfrac{\mathcal{B}(B \to D^{(*)}\tau\nu)}{\mathcal{B}(B \to D^{(*)}\ell\nu)}$, where $\ell = e, \mu$. The combined result from Belle [3–5], BaBar [6], and LHCb [7, 8] has a tension of 3.1σ with

*e-mail: seema.choudhury@kek.jp

SM [9]. The LFU test can also be performed by measuring $R(X) = \dfrac{\mathcal{B}(B \to X\tau\nu)}{\mathcal{B}(B \to X\ell\nu)}$, which is the complimentary measurement to $\mathcal{R}(D^{(*)})$ via inclusive reconstruction. The $R(X)$ measurement is more challenging due to the background from a less constrained X system. The LFU can be tested using light leptons by measuring $R(X_{e/\mu})$.

2.1 Measurement of LFU in $B^0 \to D^{*-}\ell\nu_\ell$ at Belle

Belle [10] has performed the LFU measurement in exclusive semileptonic B decay using $B^0 \to D^{*-}(\bar{D}^0(K^+\pi^-)\pi^-)\ell\nu_\ell$ decay with a data sample of 711 fb^{-1}. The analysis is done using an untagged approach, leading to high efficiency with a sizable background. The background from fake D^* is suppressed by constraining D^* momentum in the CM frame to be < 2.45 GeV/c. The signal yield is extracted with a 3-dimensional binned maximum likelihood (ML) fit to $\cos\theta_{B,D^*\ell}$ ($\frac{2E^*_B E^*_{D^*\ell} - m^2_B - m^2_{D^*\ell}}{2|p^*_B||p^*_{D^*\ell}|}$), $\Delta M = M(D^* - D^0)$, and lepton momentum (p_ℓ). The results are shown in Fig. 1. The ratio of the branching fractions of modes with electrons

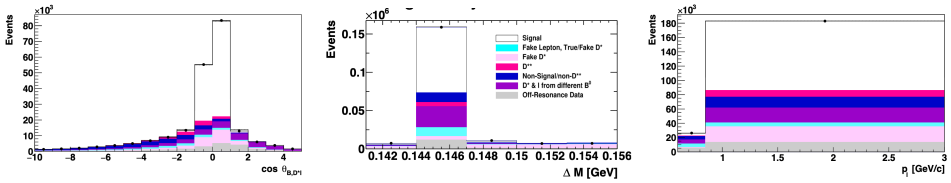

Figure 1. Fits to the $\cos\theta_B$ (left), ΔM (middle), and p_ℓ (right) in the μ mode. The points represent the data.

and muons provides a test of the LFU, *i.e.*, $\dfrac{\mathcal{B}(B^0 \to D^{*-}e^+\nu_e)}{\mathcal{B}(B^0 \to D^{*-}\mu^+\nu_\mu)} = 1.01 \pm 0.01 \pm 0.03$. The result is consistent with unity within the uncertainty.

2.2 Measurement of $\mathcal{R}(D)$ & $\mathcal{R}(D^*)$ at Belle

Belle [5] has measured simultaneously $\mathcal{R}(D)$ and $\mathcal{R}(D^*)$ using the semileptonic tagging method. Here, the tag-side B is reconstructed via $B^{0/\pm} \to D^{(*)}\ell^-\nu$ decay and signal side B from $B^{0/\pm} \to D^{(*)}\tau^-(\ell^-\bar{\nu}\nu)\nu$, the normalization channel is $B^{0/\pm} \to D^{(*)}\ell^-\nu$. The tagging method ensures good signal purity at the cost of lower signal reconstruction efficiency. The signal is extracted with 2-dimensional binned ML fit to the energies of neutral clusters detected in the ECL that are not associated with any reconstructed particles (E_{ECL}) and the background suppression classifier output ($O_{\rm cls}$). The fit results are shown in Fig. 2. The measured value of $\mathcal{R}(D) = 0.307 \pm 0.037 \pm 0.016$ and $\mathcal{R}(D^*) = 0.283 \pm 0.018 \pm 0.014$ have deviations of 0.2σ and 1.1σ, respectively. The combined result of $\mathcal{R}(D)$ & $\mathcal{R}(D^*)$ has a deviation of 0.8σ.

2.3 Measurement of $R(X_{e/\mu})$ at Belle II

Belle II [11] has checked the LFU by inclusive measurement of $R(X_{e/\mu})$ using 189 fb^{-1} of data sample with hadronic-B tagging approach. In this measurement, the signal side B flavor and kinematics in constrained by tagging the other B in its fully hadronic decays, which leads to good signal purity at a cost of lower signal reconstruction efficiency. The X system on the

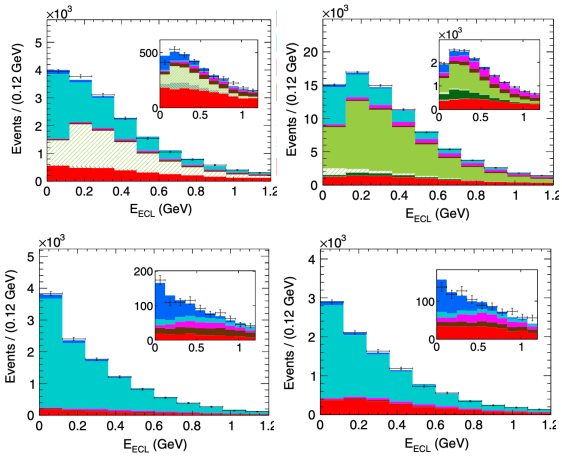

Figure 2. $E_{\rm ECL}$ fit projection and data points with statistical uncertainties in the $D^+\ell^-$ (top-left), $D^0\ell^-$ (top-right), $D^{*+}\ell^-$ (bottom-left), and $D^{*0}\ell^-$ (bottom-right) samples. The signal enhanced region is shown in the inset.

signal side contains a large variety of different charged and neutral final-state particles. As we reconstruct only the lepton in the signal side, the lepton momentum in the B signal rest frame, p^*_ℓ, is used to extract the signal yield. We required the lepton to have a high probability to be an electron or muon and $p^*_\ell > 1.3$ GeV/c to suppress backgrounds from hadrons faking as leptons and secondary leptons from $b \to c \to (\ell, s)$ cascades and $B \to X\tau\nu$. The signal yields for $B \to Xe\nu$ and $B \to X\mu\nu$ channels are extracted simultaneously in 10 bins of p^*_ℓ, with one-dimensional binned ML fit. The fit results are shown in Fig. 3. There are 48034 ± 286,

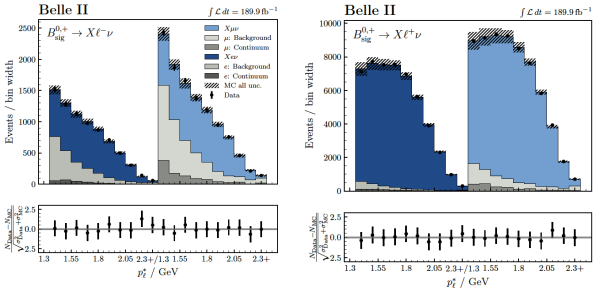

Figure 3. Distributions of Lepton momentum in the $B_{\rm sig}$ frame (p^*_ℓ) in the correct sign (left) and wrong sign (right). The electron and muon templates are fitted simultaneously in $10p^*_\ell$ bins with a width of 100 MeV each covering a p^*_ℓ range from 1.3 GeV to 2.3 GeV.

58569 ± 429 signal events for $B \to Xe\nu$ and $B \to X\mu\nu$ channels, respectively. The $R(X_{e/\mu})$ measured to be 1.033 ± 0.010 ± 0.020, for $p^*_\ell > 1.3$ GeV/c. This is the first inclusive test of (e, μ) lepton flavor universality in semileptonic $B \to X\ell\nu$ decays. The measurement is in agreement with unity within 1.5σ, with a world-leading precision of 2.2%. This measurement paved the path for $R(X) = R(X_{\tau/\ell})$ measurement.

3 LFU in $b \to s$ transition

$b \to s$ is propagated through loop-level transition and are important probe to test the LFU by measuring R_K and R_{K^*} for $B \to K\ell\ell$ and $B \to K^*\ell\ell$ decays, *i.e.*, $R_{K^{(*)}} = \dfrac{\mathcal{B}(B \to K^{(*)}\mu\mu)}{\mathcal{B}(B \to K^{(*)}ee)}$. According to SM this ratio should be 1 [12], as the coupling of leptons to gauge boson is independent of flavor. LHCb [13] has reported a deviation of 3.1σ in R_{K^+} measurement for $q^2 \in [1.1 - 6.0]$ GeV$^2/c^4$ bin using 9 fb^{-1} data sample, q^2 is invariant mass square of lepton pair. Similarly, $R_{K^{*+}}$ and $R_{K^0_S}$ measurements from LHCb [14] have 1.4σ and 1.5σ deviations from SM, calculated in 3 fb^{-1} data sample.

3.1 R_{K^*} measurement at Belle

Belle [15] has measured R_{K^*} using a full data sample of 711 fb^{-1}. The decay modes reconstructed are $B^+ \to K^{*+}(K^+\pi^0, K^0_S\pi^+)\ell\ell$ and $B^0 \to K^{*0}(K^+\pi^-, K^0_S\pi^0)\ell\ell$. The kinematic variables which distinguish the signal from the background are beam-energy-constrained mass, $M_{\rm bc} = \sqrt{E^2_{beam}/c^4 - |p_B|^2/c^2}$ and energy difference, $\Delta E = E_B - E_{beam}$. Here, p_B and E_B are the momentum and energy of the B candidate, and E_{beam} is the beam energy. The background coming from the continuum and $B\bar{B}$ are suppressed using Neural Network (NN). The signal yield is obtained by performing a 1-dimensional unbinned extended ML fit in $M_{\rm bc}$, shown in Fig. 4. From the fit, the signal yields are $103^{+13.4}_{-12.7}$ and $139.9^{+16.0}_{-15.4}$ for electron and muon channels, respectively. From the fitted signal yield and signal MC efficiency, the R_{K^*} is cal-

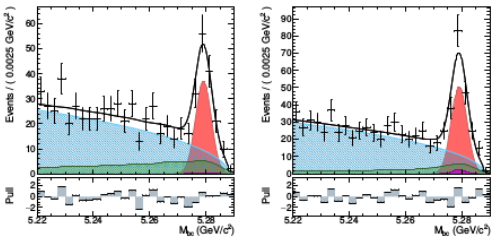

Figure 4. Fit result of $B \to K^*\ell\ell$ in terms of $M_{\rm bc}$ for the electron (left) and muon (right) modes with $q^2 > 0.045$ GeV$^2/c^4$. Combinatorial (dashed blue), signal (red filled), charmonium (dashed green), peaking (purple dotted), and total (solid) fit distributions are superimposed on data (points with error bars).

culated for charged B, neutral B, and the combined result from charged and neutral B, as shown in Fig. 5. The results for different bins are consistent with SM expectations within the uncertainty.

3.2 R_K measurement at Belle

R_K tests LFU in $B \to K\ell\ell$ decays. The analysis is performed in 711 fb^{-1} data sample of Belle [16]. The decay modes reconstructed are $B^+ \to K^+\ell\ell$ and $B^0 \to K^0_S\ell\ell$. The background from continuum and $B\bar{B}$ are suppressed using a NN which uses several event shapes, vertex quality, and kinematic variables. The signal yield is extracted by 3-dimensional unbinned extended ML fit in $M_{\rm bc}$, ΔE, and the translated NN output ($\mathcal{O}'$). The fit results are shown in

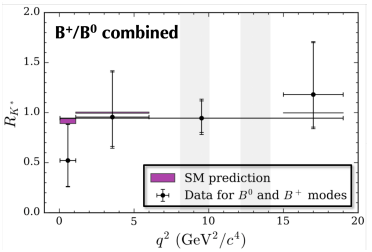

Figure 5. Result for R_{K^*} compared to SM predictions in bins of $q^2 \in [0.045, 1.1]$, $[1.1, 6]$, $[15, 19]$, and $[0.045, 19]$ GeV$^2/c^4$. The shaded bands indicate the charmonium vetoes.

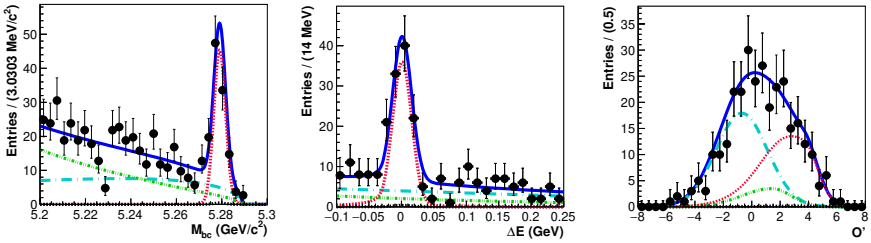

Figure 6. Signal-enhanced $M_{\rm bc}$ (left), ΔE (middle), and $\mathcal{O}'$ (right) projections for $B^+ \to K^+\mu\mu$ decay. Point with error bars are the data, blue solid curves are the fitted result, red dashed curves denote the signal component, cyan long dashed, green dash-dotted, and black dashed curves represent continuum, $B\bar{B}$ background, and $B \to$ charmless decays, respectively.

Fig. 6. There are 137 ± 14, 138 ± 15, $27.3^{+6.6}_{-5.8}$, and $21.8^{+7.0}_{-6.1}$ signal events for $B^+ \to K^+\mu\mu$, $B^+ \to K^+ee$, $B^0 \to K^0_S\mu\mu$, and $B^0 \to K^0_S ee$, respectively. The R_{K^+}, R_{K^0}, and R_K are measured in different q^2 bins, as shown in Fig. 7. The results are in agreement with SM expectations within the uncertainty. In addition to this, we have the most precise measurement for R_K in the J/ψ region and is consistent with the unity, *i.e.*, $R_{K^+}(J/\psi) = 0.994 \pm 0.011 \pm 0.010$ and $R_{K^0}(J/\psi) = 0.993 \pm 0.015 \pm 0.010$.

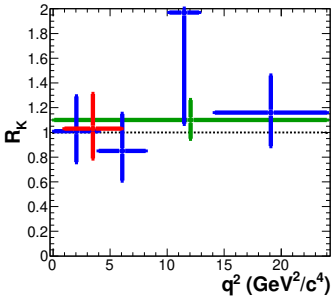

Figure 7. R_K in bins of q^2 for $B \to K\ell\ell$. The red marker represents the bin of $1.0 < q^2 < 6.0$ GeV$^2/c^4$, and the blue marker are for $0.1 < q^2 < 4.0$, $4.00 < q^2 < 8.12$, $10.2 < q^2 < 12.8$, and $q^2 > 14.18$ GeV$^2/c^4$ bins. The green marker denotes the whole q^2 region excluding the charmonium resonances.

3.3 Measurement of $\mathcal{B}(B \to K^*\ell\ell)$ at Belle II

Belle II [17] has measured $\mathcal{B}(B \to K^*\ell\ell)$ using 190 fb^{-1} of data. For this analysis, the decay modes reconstructed are $B^0 \to K^{*0}(K^+\pi^-)\ell\ell$ and $B^+ \to K^{*+}(K^+\pi^0, K^0_S\pi^+)\ell\ell$. The signal yield is extracted by 2-dimensional un-binned extended ML fit in $M_{\rm bc}$ and ΔE for the events which pass tight requirement on the boosted decision tree [18], used to fight the background from continuum and $B\bar{B}$. The fit results are shown in Fig. 8. The branching fractions are

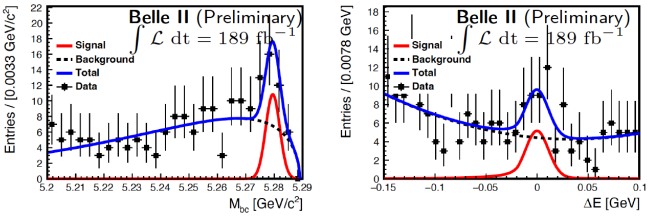

Figure 8. $M_{\rm bc}$ (left) and ΔE (right) projection for $B \to K^*\ell\ell$ decay. Points with error bars are superimposed on the blue (solid) curve showing total fit result, while red (solid) and black (dotted) lines represent the signal and background components.

measured for the entire range of the dilepton mass, excluding the mass region to suppress the $B \to K^*\gamma(\to e^+e^-)$ background and the regions compatible with decays of charmonium resonances to be; $\mathcal{B}(B \to K^*(892)\mu^+\mu^-) = (1.19 \pm 0.31^{+0.08}_{-0.07}) \times 10^{-6}$, $\mathcal{B}(B \to K^*(892)e^+e^-) = (1.42 \pm 0.48 \pm 0.09) \times 10^{-6}$, and $\mathcal{B}(B \to K^*(892)\ell^+\ell^-) = (1.25 \pm 0.30^{+0.08}_{-0.07}) \times 10^{-6}$. The results are compatible with the world averages within the uncertainties. This is a preliminary step towards the LFU test using larger data sample of Belle II.

3.4 Measurement of $R_K(J/\psi)$ at Belle II

Belle II [19] has tested LFU in $B \to J/\psi K$ using 190 fb^{-1} data sample. The decay modes reconstructed are $B^+ \to J/\psi(\ell\ell)K^+$ and $B^0 \to J/\psi(\ell\ell)K^0$. The signal yield is obtained by 2-dimensional un-binned extended ML fit in $M_{\rm bc}$ and ΔE. The fit results are shown in Fig. 9. The signal has a purity of 90 – 95%. The LFU ratio measured from charged and neutral B are $R_{K^+}(J/\psi) = 1.009 \pm 0.022 \pm 0.008$ and $R_{K^0}(J/\psi) = 1.042 \pm 0.042 \pm 0.008$, respectively. These results are statistically dominated and in agreement with PDG [20].

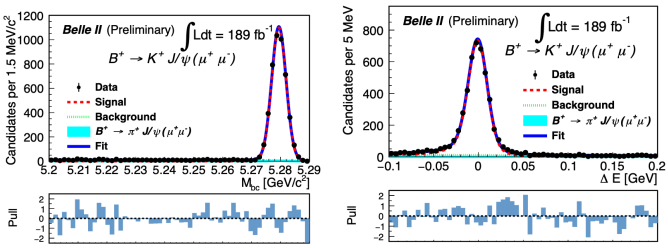

Figure 9. $M_{\rm bc}$ (left) and ΔE (right) distributions with the fit result superimposed. Black dots with error bars denote the data, blue curve denote the total fit, dashed red curves are the signal component, dotted green curves are the background component, and filled cyan regions are the $B^+ \to J/\psi\pi^+$ component.

4 Measurement of $R(\Omega)$ at Belle

LFU in Ω_c^0 is probed for the first time with $\Omega_c^0 \to \Omega^- \ell^+ \nu_\ell$ decay using Belle [21] data sample of 922 fb^{-1}. The data 89.5, 711, and 121.1 fb^{-1} are collected at the CM energies of 10.52, 10.58, and 10.86 GeV, respectively. These decays are reconstructed in the process $e^+e^- \to c\bar{c} \to \Omega_c^0 + anything$. The signal yield is extracted by binned ML fit to the invariant mass ($M_{\Omega\ell}$) spectra. The fit results are shown in Fig. 10. The signal yield for $\Omega_c^0 \to \Omega^-\pi^+$, $\Omega_c^0 \to \Omega^- e^+ \nu_e$, and $\Omega_c^0 \to \Omega^-\mu^+\nu_\mu$ are 865.3 ± 35.3, 707.6 ± 37.7, and 367.9 ± 31.4, respectively. The significance of the $\Omega_c^0 \to \Omega^-\ell^+\nu_\ell$ are both larger than 10σ, and $\Omega_c^0 \to \Omega^-\mu^+\nu_\ell$ decay is seen for the first time in Belle, where $\Omega_c^0 \to \Omega^-\pi^+$ decay is used as a normalization channel. The

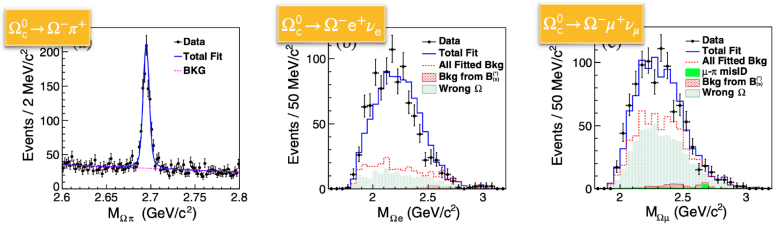

Figure 10. Fit to the $M_{\Omega\pi}$ (left), $M_{\Omega e}$ (middle), $M_{\Omega\mu}$ (right) distributions. The dots with error bars represent the data, the solid lines are the best fits, and the dashed lines are the fitted total background. The blank areas between the red dashed lines and shaded histograms are from backgrounds with misselected ℓ^+. The $\mu - \pi$ misID in $M_{\Omega\mu}$ plot is the background from $\Omega_c^0 \to \Omega^-\pi^+ + hadrons$ decays.

semileptonic decay branching fraction ratio is calculated to be; $R(\Omega) = \dfrac{\mathcal{B}(\Omega_c^0 \to \Omega^- e^+ \nu_e)}{\mathcal{B}(\Omega_c^0 \to \Omega^-\mu^+\nu_\mu)} = 1.02 \pm 0.10 \pm 0.02$. The $R(\Omega)$ agrees with the expected LFU value 1.03 ± 0.06 [22] within the uncertainty.

5 LFU prospects at Belle II

The $R(X)$ measurement or in general inclusive processes are unique to Belle II. The estimated precision on $R(X)$ for 189 fb^{-1} of data sample is $\sim$ 17%. The uncertainty (statistical + systematic) projections for $\mathcal{R}(D)$, $\mathcal{R}(D^*)$, and $R(X)$ are shown in Fig. 11 [23]. A few ab^{-1} of data from Belle II will be sufficient to track the anomaly on $\mathcal{R}(D) - \mathcal{R}(D^*)$ to be statistical or systematic origin. With the full data sample of Belle II, the total uncertainty for $\mathcal{R}(D) - \mathcal{R}(D^*)$ will be $2-3\%$ for different tagging approaches (semileptonic or hadronic). $R(X)$ will also be of similar precision. Similarly, for $b \to s$ transition, the R_{K^*} projections for 1 ab^{-1}, 5 ab^{-1}, and 50 ab^{-1} are shown in Fig. 11. The R_{K^+} and R_{K^*} statistical sensitivity will be $< 2\%$ for the entire q^2 region and $\sim 3\%$ for $q^2 \in [1-6]$ GeV$^2/c^4$, with full data sample of 50 ab^{-1}. Contrary to LHCb, Belle II can check these observables both for low and high q^2 bins. Belle II will provide an independent measurement to confirm the tension observed in $R_K - R_{K^*}$ with few ab^{-1} of data sample.

6 Summary

The flavor physics in e^+e^- collisions offers an extremely rich physics program with many opportunities to probe physics beyond the SM. At Belle II, we can access charged and neutral B with equal efficiency and also have equal sensitivity for electron and muon channels.

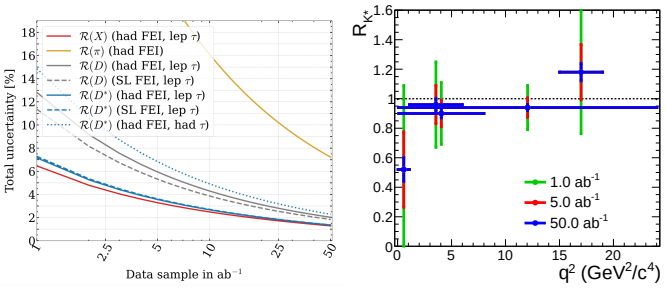

Figure 11. LFU prospects of Belle II for $b \to c$ (left) and $b \to s$ (right) transitions.

Belle II can access inclusive decay modes in addition to exclusive decays, and analysis can be performed in tagged or un-tagged approaches. Belle II has collected $\sim$ 424 fb^{-1} of data which is comparable to the size of the BaBar data sample and can be combined with the Belle data sample to increase statistics. So far, Belle or Belle II have not observed any sign of LFU violation and a higher data sample will shed light on LFU anomalies. Some results show the potential of Belle II, and only a part of them are covered here. We will have more results from Belle II in near future.

References

[1] A. Abashian *et al.* (Belle Collaboration), NIMPR Sec. A 479, **117** (2002); also, see the detector section in J. Brodzicka et al., PTEP 2012, **04D001** (2012).
[2] T. Abe *et al.* (Belle II Collaboration), arXiv:1011.0352.
[3] M. Huschle *et al.* (Belle Collaboration), PRD 92, **072014** (2015).
[4] S. Hirose *et al.* (Belle Collaboration), PRL 118, **211801** (2017).
[5] G. Caria *et al.* (Belle Collaboration), PRL **124** 161803 (2020).
[6] J. P. Lees *et al.* (BaBar Collaboration), PRD 88, **072012** (2013).
[7] R. Aaij *et al.* (LHCb Collaboration), PRL **115**, 111803 (2015).
[8] R. Aaij *et al.* (LHCb Collaboration), PRD **97**, 072013 (2018)].
[9] Y. Amhis *et al.* (HFLAV Collaboration), arXiv:2206.07501.
[10] E. Waheed *et al.* (Belle Collaboration), PRD **100**, 052007 (2019).
[11] H. Junkerkalefeld *et al.* (Belle II Collaboration), ICHEP 2022.
[12] M. Bordone, G. Isidori, and A. Pattori, EPJC **76**, 440 (2016).
[13] R, Aaji *et al.* (LHCb Collaboration), Nature Physics **18**, 277 (2022).
[14] A. Aaij *et al.* (LHCb Collaboration), PRL **128**, 191802 (2022)].
[15] S. Wehle *et al.* (Belle Collaboration), PRL 126, 161801 (2021).
[16] S. Choudhury *et al.* (Belle Collaboration), JHEP **03**, 105 (2021)
[17] F. Abudinén *et al.* (Belle II Collaboration), arXiv:2206.05946.
[18] T. Keck, arXiv:1609.06119.
[19] F. Abudinén *et al.* (Belle II Collaboration), arXiv:2207.11275.
[20] P.A. Zyla *et al.* (Particle Data Group), PTEP 2020, **083C01** (2020).
[21] Y. B. Li *et al.* (Belle Collaboration), PRD **105**, L091101 (2022).
[22] F. Huang, Q. A. Zhang, arXiv:2108.06110.
[23] Snowmass 2021, Belle II Physics for Snowmass.